MEAN-SHIFT BASED ALGORITHM FOR THE MEASUREMENT OF BLOOD GLUCOSE IN HAND-HELD DEVICES

Nevine Demitri and Abdelhak M. Zoubir

Signal Processing Group, Institute of Telecommunications
Technische Universität Darmstadt, Merckstr. 25, 64283
Darmstadt, Germany
{ndemitri, zoubir}@spg.tu-darmstadt.de

ABSTRACT

We propose an algorithm to estimate the glucose concentration from a very small blood sample in a novel hand-held measurement device. A photometric measurement system is used whereby a camera is employed to observe the reflectance behavior of the chemical reaction. The aim is to estimate and track this behavior in the region of interest. The approach is based on mode tracking via the adaptive mean-shift algorithm, using both spatial and range information. Finally, the estimated glucose concentration is associated with the obtained mode. We show that binning the images increases the mode detection accuracy. Using both synthetic and real data, we validate the proposed algorithm.

Index Terms— Adaptive mean-shift, blood glucose measurement, segmentation.

1. INTRODUCTION

According to the World Health Organization (WHO) [1], the burden of diabetes is increasing globally, with 347 million diabetics worldwide in 2012. Complications of diabetes such as blindness and heart diseases can be delayed, or even prevented by careful monitoring. For this purpose, glucose biosensors are integrated in hand-held invasive devices that enable a regular self-monitoring by the patient.

We use devices that operate on a novel photometric measurement principle that uses a much smaller blood sample than is typical for state of the art devices. Here, the glucose in the blood sample, which is applied to a chemical test strip, reacts with the chemical agent, leading to a color change. This color change is tracked optically and the resulting convergence value is related to the actual glucose concentration. The optical tracking is performed using a camera that captures both the regions where the chemical reaction has taken place and the surrounding areas. Using methods of image segmentation, we can find the region of interest (ROI) which contains the reaction between the chemical agent and the glucose. Then, we estimate the glucose concentration, which is related to the intensity of the ROI.
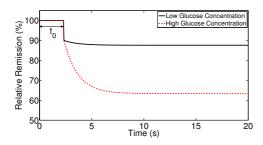
In many cases, such as low glucose cases, standard intensity-based segmentation techniques fail to find the region of interest reliably, especially if artifacts are present in the images. Therefore, mean-shift clustering presents a good solution. It was originally introduced by Fukunaga and Hostetler in [2]. Recently, it was re-adopted by Cheng [3] and generalized as a gradient ascent method with adaptive step size. Comaniciu and Meer applied the mean-shift algorithm [4] to low-level vision problem, such as segmentation. It has recently become a popular tool for segmentation of biomedical images [5, 6]. Mean-shift clustering is an unsupervised non-parametric clustering approach that analyzes the empirical probability density function and locates its modes, taking into account both intensity-based and spatial information in the image. One of its major advantages is that it does not require an initialization of the number of clusters or their positions. This characteristic is beneficial for our application as we want to temporally track images of the chemical reaction, which may lead to the number of clusters changing over time.

Our contributions lie in proposing an unsupervised mean-shift based algorithm that reliably estimates the glucose concentration, regardless of artifacts corrupting the image. To our knowledge this paper is the first to tackle the problem of vision based estimation of blood glucose concentrations. Furthermore, we show that binning the images prior to segmentation, improves the performance.

The remainder of the paper is organized as follows: Section 2 explains the photometric measurement principle. The mean-shift algorithm is described in Section 3. The proposed algorithm is presented in Section 4, followed by the description of the data set and the results in Section 5. Finally, a conclusion is given in Section 6.

2. PHOTOMETRIC MEASUREMENT PRINCIPLE FOR BLOOD GLUCOMETRY

The photometric measurement principle is a common principle to measure the concentration of an analyte in a fluid, such

Fig. 1: An idealized model of the temporal behavior of the chemical reaction for high and low glucose concentrations.

as the concentration of glucose in a blood sample. It relies on a chemical reaction between the analyte and a chemical agent on a test strip that yields a change of color [7]. The test strip is then illuminated and the reflected light detected, providing information on the concentration of the analyte. The reflectance behavior is observed using a camera that produces 30 frames per second. The amount of reflected light is denoted relative remission R and can be directly related to the glucose concentration value, knowing the corresponding mapping function. A resolution $\Delta R = 0.1$ is needed to differentiate between two distinct glucose concentration values. To determine the convergence value of the reaction, the temporal development of R has to be tracked. It can be, typically, subdivided into three stages as depicted in Fig. 1.

1. Constant intensity stage where the reaction between the glucose and the chemical agent has not started.
2. The moistening period starts at $t = t_0$ and is characterized by a rapid drop of the intensity value.
3. The convergence stage shows a slow decrease of the intensity, which can be modeled by an exponential decay.

The images, obtained during the first stage, are referred to as light images and serve as a reference for normalization of all consequent measurements. A set of so-called dark images is taken before the test field enters the observation area of the camera. These are used for calibration.

Fig. 2 shows examples of the observations obtained by the camera at different stages and for different time instances as well as their corresponding histograms. Typically, the frames show a yellow/orange region corresponding to the test strip on a dark red background. The initial histogram (Fig. 2(d)) obtained at $t < t_0$ can, therefore, be characterized by three main areas corresponding to the background, the test strip and the border of the test strip. Fig. 2(b) and (c) exemplify the observations after convergence ($t > t_C$) for low and high glucose values, respectively. The high glucose case shows a much more pronounced color change in the reaction region. Naturally, the higher the glucose concentration the stronger is the color change w.r.t. the initial reflectance (cf. Fig. 1). Also, visible in Fig. 2(b) is that the reaction is confined to a vertically rectangular shaped region in the middle of the

test strip. The corresponding histograms in Fig. 2(e) and (f) demonstrate the following: proceeding in time a fourth mode develops and moves from the high intensity region in the direction of the lower intensity region, with its final mode position depending on the relative remission value. Appearing artifacts may lead to further modes developing, so that the actual mode number is unknown and changes over time. This behavior motivates the use of the mean-shift algorithm as it will be explained in the following section.
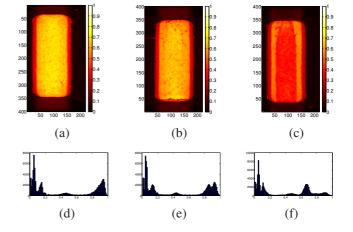

Fig. 2: Examples of the chemical reaction observed by the camera and the corresponding histograms. Figures (a) and (d) show an example at $t < t_0$, (b) and (c) show observations of $t > t_C$ for low and high glucose values, respectively, (e) and (f) are the corresponding histograms.

3. MEAN SHIFT ALGORITHM

Given L feature vectors $\mathbf{x}_l, l = 1, \ldots, L$ in a d-dimensional space $\mathcal{R}^d$, the kernel density estimator at vector $\mathbf{x}$ can be defined as [4]

$$\hat{f}_K(\mathbf{x}) = \frac{c}{L} \sum_{l=1}^{L} \frac{1}{\mathbf{h}^d} k\left(\left\|\frac{\mathbf{x} - \mathbf{x}_l}{\mathbf{h}}\right\|^2\right), \qquad (1)$$

where k is the profile of a radially, symmetric kernel function $K(\mathbf{x})$ such as

$$K(\mathbf{x}) = c \cdot k(\|\mathbf{x}\|^2). \qquad (2)$$

In (1), c is a constant that ensures that $K(\mathbf{x})$ integrates to one and $\mathbf{h}$ is the so-called kernel bandwidth parameter, which defines the range of the kernel. We use the following kernel:

$$K(\mathbf{x}) = \frac{1}{2\pi^{\frac{d}{2}}} e^{-\frac{\|\mathbf{x}\|^2}{2}}. \qquad (3)$$

To find the modes of the empirical probability density function, the zeros of the gradient need to be found

$$\nabla \hat{f}_K(\mathbf{x}) = \frac{2c}{L} \sum_{l=1}^{L} \frac{(\mathbf{x} - \mathbf{x}_l)}{\mathbf{h}^{d+2}} k'\left(\left\|\frac{\mathbf{x} - \mathbf{x}_l}{\mathbf{h}}\right\|^2\right), \qquad (4)$$

where $k'(\mathbf{x})$ denotes the derivative of the function $k(\mathbf{x})$. Rewriting (4) in the form

$$\nabla \hat{f}_K(\mathbf{x}) = \frac{2c}{L} \left[\sum_{l=1}^{L} \frac{1}{\mathbf{h}^{d+2}} k' \left(\left\| \frac{\mathbf{x} - \mathbf{x}_l}{\mathbf{h}} \right\|^2 \right) \right] \cdot \mathbf{m}_{\mathbf{h},k'} \quad (5)$$

yields the mean-shift vector as

$$\mathbf{m}_{\mathbf{h},k'}(\mathbf{x}) = \left[\frac{\sum_{l=1}^{L} \frac{1}{\mathbf{h}^{d+2}} \mathbf{x}_l k' \left(\left\| \frac{\mathbf{x} - \mathbf{x}_l}{\mathbf{h}} \right\|^2 \right)}{\sum_{l=1}^{L} \frac{1}{\mathbf{h}^{d+2}} k' \left(\left\| \frac{\mathbf{x} - \mathbf{x}_l}{\mathbf{h}} \right\|^2 \right)} - \mathbf{x} \right] . \quad (6)$$

The mean-shift vector can be, intuitively, understood as the difference between the weighted mean and the center of the kernel $\mathbf{x}$. Due to (4), it always moves in the direction of the steepest ascent. The step-size of the movement is determined by the magnitude of the mean-shift vector. It is large for points with low local density and small for points with high local density. The mean-shift vector reaches convergence when its magnitude becomes zero, indicating a stationary point.

The mean-shift algorithm iterates through each feature vector $\mathbf{x}_l$ in the data set, performing the following steps:

- Calculate the mean-shift vector $\mathbf{m}_{\mathbf{h},k'}(\mathbf{x}_l^j)$ of current feature vector $\mathbf{x}_l^j$, where j is the iteration variable.
- Shift the vector $\mathbf{x}_l^j$ towards $\mathbf{m}_{\mathbf{h},k'}(\mathbf{x}_l^j)$, hereby calculating the next iteration point $\mathbf{x}_l^{j+1} = \mathbf{x}_l^j + \mathbf{m}_{\mathbf{h},k'}(\mathbf{x}_l^j)$.
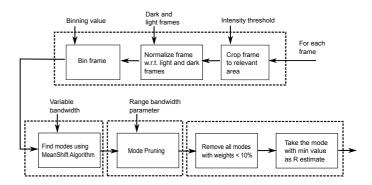- Stop when convergence is reached, i.e. $|\mathbf{x}_l^{j+1} - \mathbf{x}_l^j| < \epsilon$.

The mean-shift algorithm does not require information about the clusters, such as their number and positions, which motivates our choice of it. In fact, the only parameter to be set is the bandwidth parameter $\mathbf{h}$. Choosing a high $\mathbf{h}$ leads to peaks being smoothed out, while choosing a small $\mathbf{h}$ leads to an over representation of the tails of the density. It is, thus, beneficial to use a data-driven bandwidth parameter that adapts to the current feature vector. We apply the variable bandwidth parameter suggested by Comaniciu *et. al* in [8]:

$$\mathbf{h}(\mathbf{x}) = \mathbf{h}_0 \left[\frac{\lambda}{\hat{f}(\mathbf{x})} \right]^{\frac{1}{2}} . \quad (7)$$

Here, $\mathbf{h}_0$ is an initial fixed bandwidth, λ is the geometric mean of an initial estimate of the probability density and $\hat{f}(\mathbf{x})$ is an estimate of the probability of the estimation point $\mathbf{x}$. Hereby, $\mathbf{h}(\mathbf{x})$ becomes larger for points with a low local density and smaller for points with a high local density.

4. PROPOSED ALGORITHM

The aim of this work is to estimate the relative remission R from a set of images that describe the reflectance behavior. For this, we developed an algorithm that is summarized in Fig. 3. The algorithm is executed for each frame to track the temporal behavior of the chemical reaction. It will be successively presented in the next sections.

Fig. 3: Flow graph illustrating the proposed algorithm.

4.1. Pre-processing Stage

The pre-processing stage consists of three main steps. The first step is to crop the images to the area of the chemical test strip, by removing all pixels lower than a threshold t_{crop} from the image. Setting t_{crop} is straightforward, as the intensity difference between the background and the test field is large. Next, a normalization is performed to ensure that no effects arise from different illumination conditions and to enhance the region of interest. It is given by

$$I_{\text{norm}}(m,n) = \frac{I_{\text{current}}(m,n) - I_{\text{dark}}(m,n)}{I_{\text{light}}(m,n) - I_{\text{dark}}(m,n)}, \quad (8)$$

where $m = 1, ..., M, n = 1, ..., N$ and M and N are the row and column sizes, respectively. $I_{\text{current}}(m,n)$ is the current image to be normalized and $I_{\text{norm}}(m,n)$ is the resulting normalized image. $I_{\text{dark}}(m,n)$ is the average of the dark images mentioned in Section 2 and $I_{\text{light}}(m,n)$ the average of the light images. Given a binning value B, the frame is, then, binned by averaging over areas of size $B \times B$ pixels.

4.2. Mean-Shift Stage

After pre-processing, the mean-shift algorithm is applied to the images. First, they are vectorized and a set of $M \cdot N$ feature vectors $\mathbf{x}_l, l = 1, ..., M \cdot N$ is built. Each feature vector is 3-dimensional and consists of $\mathbf{x}_l = [I_l, m_l, n_l]$, I_l being the intensity at point l and m_l, n_l the spatial coordinates of the image. The kernel we use, thus reads

$$K_{h_r,h_s}(\mathbf{x}) = \frac{c}{h_s^2 h_r} k \left(\left\| \frac{\mathbf{x}^s}{h_s} \right\|^2 \right) \cdot k \left(\left\| \frac{\mathbf{x}^r}{h_r} \right\|^2 \right), \quad (9)$$

h_r and h_s being the range and spatial bandwidth parameters, respectively and $\mathbf{x}^s$ and $\mathbf{x}^r$ the spatial and range components of the feature vectors. For the range bandwidth parameter h_r, we use the relation of (7) and set h_0 according to the plug-in rule [9]:

$$h_0 = 1.06 \hat{\sigma} L^{-\frac{1}{5}}, \quad (10)$$

where $\hat{\sigma}$ is an estimate of the standard deviation of the intensity information. The spatial bandwidth is set to a fixed value

h_s, depending on the image size. The convergence constant is set to $\epsilon = 0.05$, as this is half the needed resolution ΔR to distinguish between different glucose concentrations. The mean-shift algorithm results in a set of modes $\mathbf{y}$ of size $M \cdot N$.

4.3. Mode Pruning Stage

As the mean-shift algorithm typically yields more modes than actually exist, a mode pruning step is required to reduce the number of modes to the relevant ones. This stage only takes into account the intensity characteristics of the pixels for clustering. The mode pruning consists of the subsequent steps:

- Initialize the first mode in the vector as the first cluster.
- Iterate through the resulting modes vector $\mathbf{y}$.
- If the next mode is further than h_0 (from(10)) to the first cluster, assign it to be a new cluster. Otherwise, assign it to an existing cluster and update the cluster.
- Repeat until all points in the vector $\mathbf{y}$ have been assigned to a cluster.

As a result all modes, which are close to each other, are grouped together to one cluster, hereby, reducing the amount of modes considerably.

4.4. Relative Remission Estimation Stage

The output of the mode pruning stage is a set of few modes. For each of these modes, a weight is assigned depending on the number of pixels ascribed to this mode. If the weight is smaller than the threshold $t_{\mathrm{modes}} = 0.1$, the mode is not considered as an estimate of the glucose concentration. t_{modes} was empirically determined by evaluating typical mode weights for different regions in the images. We are now, ideally, left with a set of two modes. These can be associated with the region of interest and the dry test field area. The mode with the smaller intensity value is assigned to the region of interest and is taken to be the estimate of the relative remission $\widehat{R}$, as it, typically, has a lower intensity value than the dry area.

5. EXPERIMENTAL RESULTS

5.1. Data Set

For testing purposes, we use both real and synthetic data. The real data set consists of 48 measurements performed using the system described in Section 2. Whole blood samples of five different known glucose levels are used: 30 mg/dl, 90 mg/dl, 150 mg/dl, 350 mg/dl, 550 mg/dl. Each measurement contains 605 frames, corresponding to a testing time of $t_{\mathrm{test}} = 20\,s$. The first five frames are dark frames and the consecutive 27 frames are light frames. These are used for normalization, as described in Section 4.1.

The relation between the relative remission value and the actual glucose concentration is dependent on the chemical test agent used and was not available to the authors. Consequently, a comparison of the results to a ground truth is not possible. Therefore, a synthetic data set was developed by creating a mask from the real data set using a frame at $t = t_0$. The area of the test strip is modulated with a model of the chemical reaction, as in Fig.1. Additive 0-mean Gaussian noise with a variance $\sigma_{\mathrm{syn}}^2 = 81$ is added to the frames, whereby σ_{syn}^2 is estimated from the real data samples. The aim of the synthetic data is to validate the algorithm in an artifact-free case, knowing the ground truth.

5.2. Results

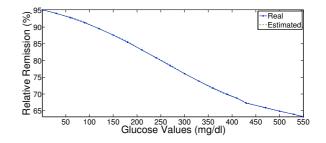#### 5.2.1. Validation using the Synthetic Data

Fig. 4: Relative remission estimates for 20 different glucose concentrations, performed using synthetic data and compared to the ground truth, using a binning value of $B = 5$.

The proposed algorithm is first validated by applying it to the synthetic data set for 20 different glucose values and 100 runs/glucose value for a binning value of $B = 5$. Fig. 4 illustrates the behavior of the true and estimated relative remission for different glucose values. The total mean squared error (MSE) is 0.001, which results in a smaller resolution ΔR than the one needed to resolve two distinct glucose values.

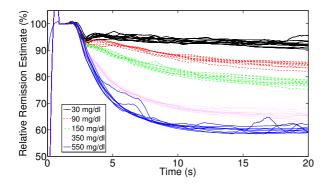#### 5.2.2. Validation using the Real Data

The results obtained using the real data are validated, by resorting to three different criteria:

1. the relative remission estimates $\widehat{R}$ for increasing glucose concentrations should be decreasing.
   Furthermore, the chemical reaction shows a higher resolution for mid field glucose concentrations.
2. the intergroup variance $\sigma_{\widehat{R}}^2$ for a measurement group of the same glucose concentration should be small.
3. the temporal behavior of the estimated relative remission values $\widehat{R}$ should match our knowledge of the temporal behavior as in Fig. 1.

Furthermore, a comparison of the mean shift based algorithm (MS) is made to the standard intensity-based Gaussian Mixture Model (GMM) - Expectation Maximization (EM) algorithm for segmentation as in [5], using two components. The

4

Gluc. val. in mg/dl	# test images	$\mu_{\widehat{R},\text{MS}}$	$\sigma^2_{\widehat{R},\text{MS}}$	$\sigma^2_{\widehat{R},\text{GMM-EM}}$
30	10	94.70	0.71	3.22
90	9	91.36	0.68	16.27
150	9	79.91	0.78	77.95
350	10	67.80	0.94	3.35
550	9	62.15	1.67	1.11

Table 1: Summary of the results with the real data set and a binning value of $B = 5$.

Fig. 5: Estimated temporal behavior of the chemical reaction for the given real data set.

results are summarized in Table 1. The third column clearly supports the fact that the mean of the estimated relative remission value $\mu_{\widehat{R},\text{MS}}$ within a test group decreases with increasing glucose concentration. Furthermore, the results show a higher resolution for the mid-field glucose values. Coming to the second criterion, we assert that the intergroup variance $\sigma^2_{\widehat{R},\text{MS}}$ is small for all glucose concentrations, especially when compared to the results $\sigma^2_{\widehat{R},\text{GMM-EM}}$ of the GMM-EM algorithm initialized with 2 clusters. This underlines the importance of using an algorithm that does not expect a fixed number of clusters. The third criterion is consolidated by Fig. 5. The performance degradation for higher glucose values is due to the chemical reaction resulting in large granular like artifacts in the ROI in these cases.

5.2.3. Data Binning

Data binning, as described in section 4.1, is performed for different binning values B. The results of the synthetic data set are evaluated in terms of the averaged MSE over tests with 20 different glucose values and 100 runs/glucose value. To assess the binning effect on the real data, the mean of the variances for each separate glucose set is computed. Table 2 presents the results, showing that binning improves the performance. Furthermore, binning reduces the computation time due to the reduced data volume. We identify the best binning value to be $B = 5$. For $B > 5$, the image structure is

lost, which leads to a degraded performance.

B	1	2	3	4	5	6
σ^2_{real}	16.2	3.73	2.03	1.62	0.96	1.19
MSE_{syn}	31.22	0.51	0.04	0.08	0.02	0.05

Table 2: Evaluation of different binning values B for both the real and synthetic data.

6. CONCLUSION

We have developed an algorithm to estimate the glucose concentration contained in a small blood sample using a photometric measurement principle to be applied in hand-held devices. It is based on adaptive mean-shift clustering, including both range and spatial information. We have shown that by applying the proposed algorithm to binned versions of the images, the accuracy improves. The validity of the algorithm was tested using both synthetic and real data and proved a good performance. We note that it is able to estimate low glucose concentrations more accurately than high glucose concentrations. To counter this, a robustification of the algorithm against artifacts is planned for future work.

7. REFERENCES

[1] "http://www.who.int/mediacentre/factsheets/fs312/en/, retrieved january 15 2013.," .

[2] K. Fukunaga and L. Hostetler, "The estimation of the gradient of a density function, with applications in pattern recognition," *IEEE Transactions on Information Theory*, vol. 21, no. 1, pp. 32–40, 1975.

[3] Yizong Cheng, "Mean shift, mode seeking, and clustering," *IEEE Transactions on Pattern Analysis and Machine Intelligence*, vol. 17, no. 8, pp. 790–799, 1995.

[4] D. Comaniciu and P. Meer, "Mean shift: a robust approach toward feature space analysis," *IEEE Transactions on Pattern Analysis and Machine Intelligence*, vol. 24, no. 5, pp. 603–619, 2002.

[5] A. Mayer and H. Greenspan, "An adaptive mean-shift framework for MRI brain segmentation," *IEEE Transactions on Medical Imaging*, vol. 28, no. 8, pp. 1238–1250, 2009.

[6] F. Sahba and A. Venetsanopoulos, "Mean shift based algorithm for mammographic breast mass detection," in *Proc. 17th IEEE Int Image Processing (ICIP) Conf*, 2010, pp. 3629–3632.

[7] Edgar Baumann, Wolfgang Obermeier, and Karl Werner, "Light source pulsed with irregular pulse sequence in analog photometric signal evaluation for a test carrier analysis system," Oct. 31 1995, US Patent 5,463,467.

[8] D. Comaniciu, V. Ramesh, and P. Meer, "The variable bandwidth mean shift and data-driven scale selection," in *Proc. Eighth IEEE Int. Conf. Computer Vision ICCV 2001*, 2001, vol. 1, pp. 438–445.

[9] Wolfgang Härdle, Axel Werwatz, Marlene Müller, and Stefan Sperlich, *Nonparametric and semiparametric models.*, Springer, 2004.